



A Case of Cholangiolocellular Carcinoma Preoperatively Diagnosed With Typical Imaging Findings

Yoshihiro Mochizuki^{1,2}, Yuji Iimuro^{1,3}, Osamu Suzuki¹, Yoji Nagashima⁴

¹Department of Surgery, Nirasaki Municipal Hospital, Nirasaki, Japan

²First Department of Surgery, University of Yamanashi, Yamanashi, Japan

³Department of Surgery, Yamanashi Prefectural Central Hospital, Yamanashi, Japan

⁴Department of Surgical Pathology, Tokyo Women's Medical University, Tokyo, Japan

Introduction: Cholangiolocellular carcinoma (CoCC) is a rare primary liver neoplasm. A recent integrative genomic analysis has revealed that CoCC represents a distinct biliary-derived molecular entity. Several cases of CoCC have been reported so far, but accurate preoperative diagnosis was difficult in most cases.

Case presentation: We report a case of 70-year-old woman with CoCC. Preoperative imaging findings revealed several typical signs of CoCC (*i.e.*, thick early ring enhancement in the peripheral area of the tumor and its prolongation, vessel penetration through the tumor, no dilatation of the peripheral bile ducts, and dot-/band-like internal enhancement or a target appearance on contrast-enhanced magnetic resonance imaging). We strongly suspected CoCC from these preoperative imaging findings of the tumor and performed extended left hepatectomy. Pathologic diagnosis was CoCC, and the histologic findings such as peripheral highly cellular areas, central abundant hyalinized/edematous fibrotic stroma, and retained Glisson's sheath structures in the tumor, corresponded closely to each preoperative imaging finding. Immunohistochemical study revealed the tumor cells were positive for cytokeratin 7 and epithelial membrane antigen. The postoperative course was uneventful, and the patient is alive without recurrence for 15 months. The prognosis of CoCC is known to be better than that of cholangiocellular carcinoma, indicating the importance of preoperative differential diagnosis of these tumors.

Conclusion: Even though preoperative diagnosis of CoCC is difficult because of its rarity, cautious investigation of preoperative typical imaging findings can possibly lead to accurate diagnosis of CoCC.

Key words: Cholangiolocellular carcinoma – Liver tumor – Imaging finding – Immunohistochemistry

Cholangiolocellular carcinoma (CoCC) is a rare primary liver neoplasm that was first reported by Steiner and Higginson in 1959.¹ CoCC is thought to originate from canals of Hering that is possibly composed of hepatic stem cells, whereas some investigators proposed the interlobular ducts as CoCC's origin.^{2,3} A recent integrative genomic analysis has revealed that CoCC represents a distinct biliary-derived molecular entity.⁴ Several cases of CoCC have been reported so far, but accurate preoperative diagnosis of CoCC was difficult in most cases because of its rarity. Meanwhile, recent analyses of imaging findings of CoCC have revealed its characteristic computed tomography (CT) or magnetic resonance imaging (MRI) findings.⁵⁻⁸ We experienced a case of liver tumor with several typical imaging findings of CoCC and strongly suspected CoCC preoperatively. Here, we present a case of CoCC with its clinical data and imaging findings, then compare the image findings with corresponding histologic data and review literature.

Case Presentation

A 70-year-old female with inactive chronic hepatitis C was referred to our hospital for an assessment of an asymptomatic liver mass that was detected by routine abdominal ultrasonography (US). She had never smoked or drunk alcohol. Laboratory data and tumor markers were within normal range, whereas anti-hepatitis C virus antibody was positive (Table 1). Abdominal US showed a well-defined, 30-mm diameter, hypoechoic mass with heterogeneous hyperechoic area inside, in segment 4 of the liver (Fig. 1a). In the Doppler mode of US, vessels penetrating the tumor were observed (Fig. 1b).

Abdominal contrast-enhanced (CE) –CT revealed an inhomogeneous thick ring-enhancement in the peripheral area of the tumor in the arterial phase (Fig. 2b). The enhancement prolonged until the delayed phase, becoming homogeneous except for the central area (Fig. 2c and 2d). Another CE-CT slice revealed vessel penetration through the tumor

in the arterial phase (Fig. 2e). In addition, no dilatation of peripheral intrahepatic bile duct was observed. ¹⁸F-fluorodeoxyglucose-positron emission tomography/CT (¹⁸F-FDG-PET/CT) revealed a weak uptake of FDG in the tumor, and the maximum standardized uptake value (SUV) was 2.83 (Fig. 2f).

In the magnetic resonance imaging (MRI) examination, the tumor showed low intensity on T1-weighted images (Fig. 3a), and heterogeneous high

Table 1 Laboratory data

	Value
WBC count, / μ L	4620
RBC count, $\times 10^4$ / μ L	446
Hb, g/dL	13.2
Hct, %	38.7
Plt, $\times 10^4$ / μ L	22.5
AST, IU/L	15
ALT, IU/L	8
ALP, IU/L	314
γ -GTP, IU/L	15
Total bilirubin, mg/dL	1
TP, g/dL	7.1
ALB, g/dL	4.1
BUN, mg/dL	9
Cre, mg/dL	0.47
Na, mEq/L	140
K, mEq/L	3.5
Cl, mEq/L	106
Ca, mg/dL	9
PT, %	89.3
APTT, s	25.5
CEA, ng/mL	0.8
CA19-9, U/mL	6.2
AFP, ng/mL	4.5
PIVKaII, U/mL	14
HBs-Ag	-
HCV-Ab	3+

AFP, alpha fetoprotein; ALB, albumin; ALT, alanine amino transferase; APTT, activated partial thromboplastin time; AST, aspartate aminotransferase; BUN, blood urea nitrogen; CA19-9, carbohydrate antigen 19-9; CEA, carcinoembryonic antigen; Cre, creatinine; Hb, hemoglobin; HBs-Ag, hepatitis B surface-antigen; Hct, hematocrit; HCV-Ab, hepatitis C virus-antibody; Na, sodium; PIVKaII, protein induced by vitamin K absence-II; Plt, platelet count; PT, prothrombin time; RBC, red blood cell; TP, total protein; WBC, white blood cell; γ GTP, gamma glutamyl-transpeptidase

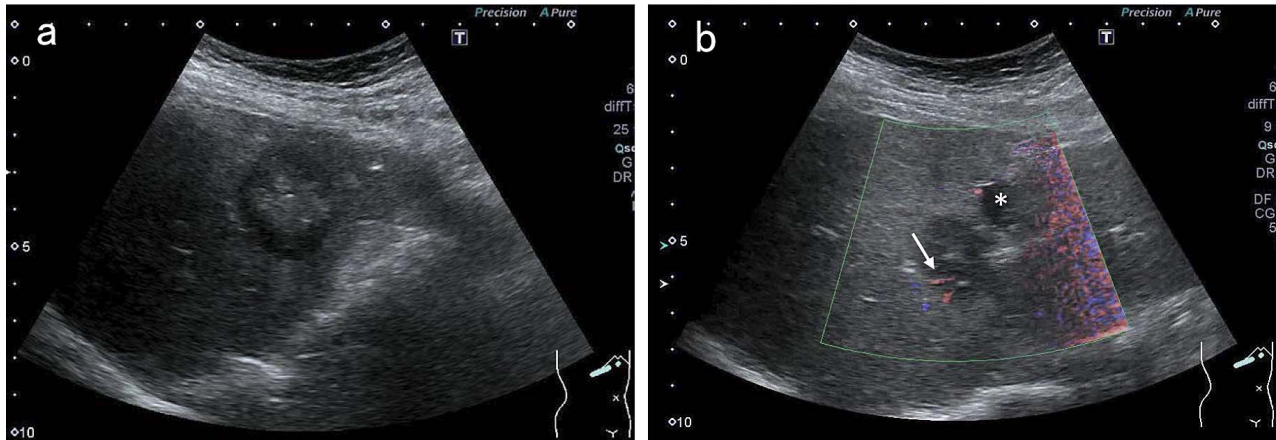


Fig. 1 Findings of abdominal ultrasonography (US). B-mode US showed a well-defined hypoechoic mass with heterogeneous hyperechoic area inside segment 4 (S4) of the liver (a). In the Doppler-mode US, vessels penetrating the tumor were detected (b, white arrow). *Adjacent liver cyst.

intensity on T2-weighted images (Fig. 3b). Dynamic MRI using the contrast agent ethoxybenzyl diethylenetriamine (EOB-MRI) revealed a pattern of tumor enhancement similar to that in the CE-CT. Namely, a thick ring enhancement appeared during the early phase (Fig. 3d), which prolonged until the

late phase (Fig. 3e). Moreover, a dot-/band-like internal enhancement during the early and late phases (Fig. 3d and 3e) and a target appearance during the hepatocyte phase (Fig. 3f), which have been reported as typical MRI findings of CoCC,⁸ were detected.

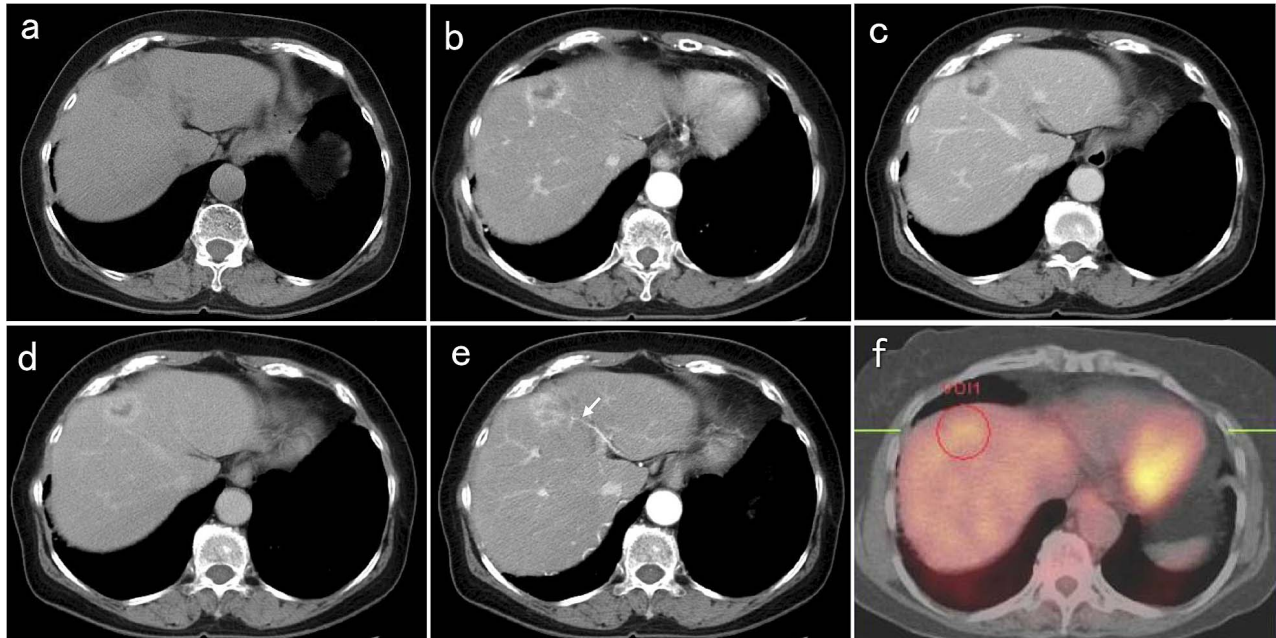


Fig. 2 Abdominal computed tomography (CT) and ¹⁸F-fluorodeoxyglucose-positron emission tomography (FDG-PET/CT). Plain CT showed a low-density area with a relatively clear boundary in the S4 (a). Contrast enhanced-CT (CE-CT) revealed an inhomogeneous thick ring-enhancement in the peripheral area of the tumor in the arterial phase (b). The enhancement prolonged until the portal (c) and delayed (d) phases, becoming homogeneous except for the central area. Another CE-CT slice revealed a finding of vessel penetration through the tumor in the arterial phase (e, arrow). FDG-PET/CT revealed only a weak uptake of FDG in the tumor with SUV max of 2.83 (f).

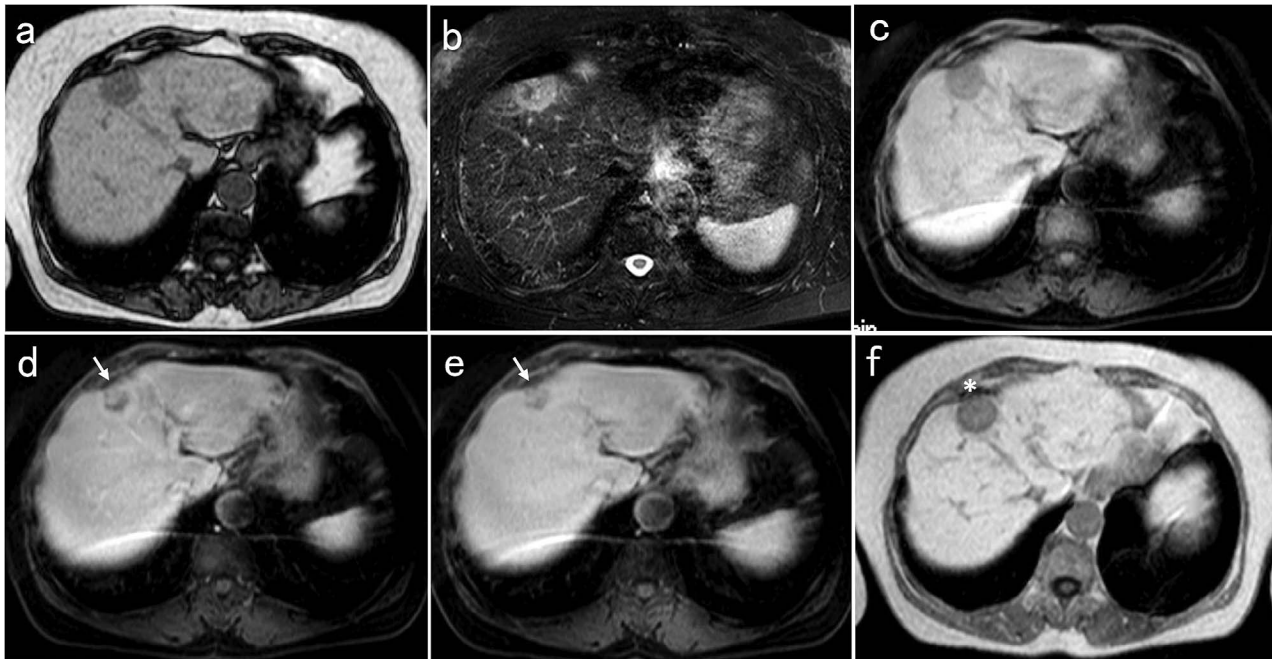


Fig. 3 Findings of magnetic resonance imaging (MRI). The tumor showed low intensity on a T1-weighted image (a) and heterogeneous high intensity on a T2-weighted image (b). In the ethoxybenzyl (EOB)-MRI, the tumor with low intensity in a plain MRI (c) showed a thick ring-enhancement during the early phase (d), and it prolonged until the late phase (e). In addition, a dot-/band-like internal enhancement during the early and late phases was detected (d, e; white arrows). The tumor showed a target appearance during the hepatocyte phase (f, asterisk).

All the imaging findings mentioned already were typical of CoCC,⁵⁻⁸ but were atypical of CCC or hepatocellular carcinoma (HCC). Therefore, we diagnosed the tumor as CoCC preoperatively, and a possible differential diagnosis was atypical CCC. The extended left hepatectomy, including the resection of the middle hepatic vein, was performed. The operating time was 285 minutes, and blood loss was 243 mL.

The resected tumor measured 45 by 30 by 20 mm and was pale yellow (Fig. 4a and 4b), and a vascular penetration through the tumor was macroscopically observed (Fig. 4b). Microscopically, the tumor comprised small tubular, acinar, or cord-like structures (Fig. 5b and 5c). The interface between the tumor and surrounding non-tumorous liver shows a replacing growth pattern of the tumor cells forming continuous tumor cords with normal liver cell cords (Fig. 5a-5c). Inside the tumor, the cells showed an “antler-like” anastomosing pattern with marked fibrous stroma that continued to the central hyalinized fibrotic stroma (Fig. 5d). In addition, retained Glisson’s sheath structures were often detected in the tumor (Fig 5a and 5b). Immunohistochemical study revealed the tumor cells were positive for

cytokeratin 7 (Fig. 6b) and negative for CK 20 (Fig. 6d). Epithelial membrane antigen (EMA) was also positive on the luminal surface of tubules of tumor cells (Fig. 6c). According to these pathologic findings of the tumor, CoCC was diagnosed. No complications occurred after operation, and the patient was discharged on postoperative day 10. She is alive without recurrence for 15 months after the operation.

Discussion

CoCC belongs to subtype of a combined HCC-CCC (CHC) with stem cell features “cholangiolocellular subtype” in the fourth version of the World Health Organization classification,⁹ and it accounts for less than 1% of all liver carcinomas. According to its classification, CoCC possibly possesses dual histologic components of HCCs and CCCs: thus, heterogeneous imaging characteristics with overlapping features of both tumors were sometimes reported.¹⁰⁻¹³

Meanwhile, recent extensive investigations of CoCC have revealed that CoCC has several characteristic image findings, and each finding closely

Table 2 Clinical features of past CoCC Cases undergoing FDG-PET

No	Author/year	Age	Sex	Background	Size (mm)	US	CT early/delay phase	MRI	PET CT SUVmax	Operation	Prognosis
1	Kadono M/2011 ¹⁴	45	F	-	75	NA	Peripheral high/high Central low/low	low on T1 high on T2	5.0	partial hepatectomy	12M alive
2	Ishii N/2015 ¹¹	59	M	-	140	low	Peripheral high/high Central low/high	low on T1 high on T2	12.8	extended right lobectomy	4M alive
3	Mori N/2016 ¹⁷	74	M	-	35	NA	Peripheral high/high Central high/high	low on T1 high on T2	25.2	right anterior segmentectomy	NA
4	Takahashi Y/2017 ¹⁵	84	M	HBV	20	low	Peripheral high/NA Central low/NA	NA	no uptake	-	NA
5	Ishii N/2017 ¹⁶	62	F	HCV	12.5	NA	Peripheral high/high Central low/high	low on T1 high on T2	4.7	Lap lateral sectionectomy	NA

CoCC, Cholangiolocellular carcinoma; CT, computed tomography; FDG-PET, fluorodeoxyglucose-positron emission tomography; MRI, magnetic resonance imaging; PET, positron emission tomography; SUV, standardized uptake value; US, ultrasound.

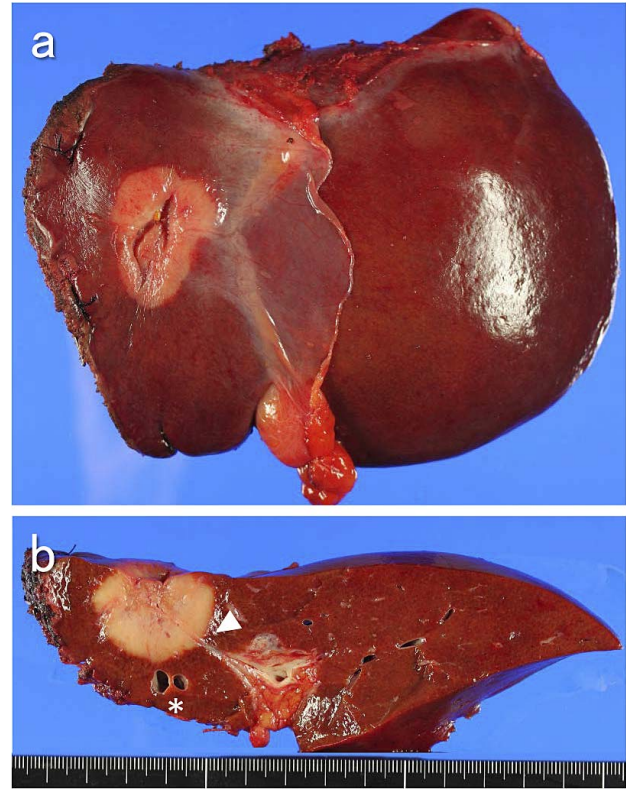


Fig. 4 Macroscopic findings of the tumor. Tumor measured 45 by 30 by 20 mm and was pale yellow (a, b), and a vascular penetration through the tumor was macroscopically observed on a cut surface of the tumor (b; white triangle). *Middle hepatic vein resected with the tumor.

corresponds to this tumor's histologic characteristic.⁵⁻⁸ In the present case, CE-CT revealed thick ring enhancement in the peripheral area of the tumor in the early phase. The enhancement prolonged until the delayed phase, becoming homogeneous except for the central area. These imaging signs are different from those observed in CCC or HCC and are thought to reflect the characteristic histologic features of CoCC (*i.e.*, many retained Glisson's sheath structures in the tumor because of replacing growth, abundant fibrous stroma in the tumor, and the central hyalinized fibrotic stroma). Replacing growth pattern of CoCC is also associated with no dilatation of peripheral intrahepatic bile ducts and the vessel-penetrating sign through the tumor. EOB-MRI revealed an enhancement pattern similar to that in the CE-CT. In addition, dot-/band-shaped internal enhancement during the arterial and portal phases was also detected. The latter findings are thought to correspond to the tumor cell nest with

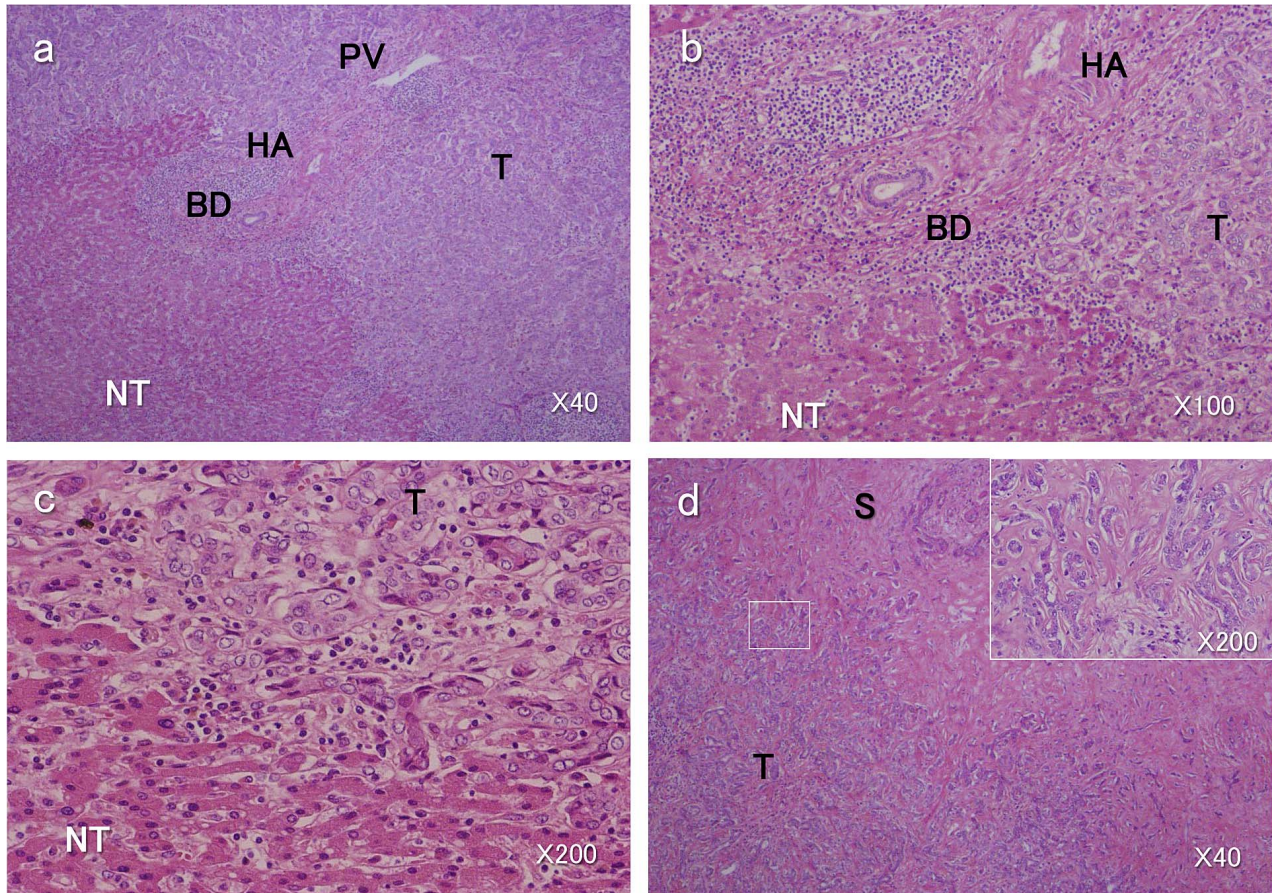


Fig. 5 Histologic findings of the tumor. The interface between the tumor (T) and surrounding non-tumorous liver (NT) showed a replacing growth pattern of the tumor cells forming continuous tumor cords with normal liver cell cords (a–c). Retained Glisson's sheath structures were often detected in the tumor (a, b). The tumor comprised small tubular, acinar, or cord-like structures (c). Inside the tumor, tumor cells showed an “antler-like” anastomosing pattern with marked fibrous stroma, which continues to the central hyalinized fibrotic stroma (d, S). BD, bile duct, HA: hepatic artery, PV: portal vein. Original magnification is indicated in each picture.

vascular proliferations and retained Glisson's sheath structures.⁸

Among the case reports of CoCC, FDG PET has been performed in only 5 cases (Table 2). In the present study, the accumulation of FDG in the tumor was relatively low, and the SUV max was 2.83. This finding was compatible with several cases reported previously,^{14–16} and the low density of tumor cells with abundant fibrous stroma in this tumor is possibly associated with the low uptake of FDG. However, a strong accumulation of FDG into the CoCC was reported in other cases,^{11,17} suggesting the diversity of tumor cell activity of CoCC. Further investigation of the relationship between FDG accumulation and tumor histology in each CoCC case is required to address these discrepancies.

Prognosis of CoCC has been reported to be better than that of CCC,^{18,19} indicating this tumor's relatively low malignant potential, while prognosis of the whole combined HCC–CCC (CHC) including a classical type, a subtype of CHC with stem cell features, an intermediate cell type, and cholangiolocellular subtype⁹ is similar to that of CCC.^{20,21} These data may indicate that CoCC and other CHC tumors belong to a distinct category.²² Indeed, a recent integrative genomic analysis has revealed that CoCC belongs to a distinct biliary molecular entity with a biliary molecular profile, low chromosomal instability, and enrichment of TGF- β and immune-related signaling.⁴ Thus, accurate preoperative diagnosis of CoCC is important for surgical planning, and adequate resection possibly leads to good prognosis.

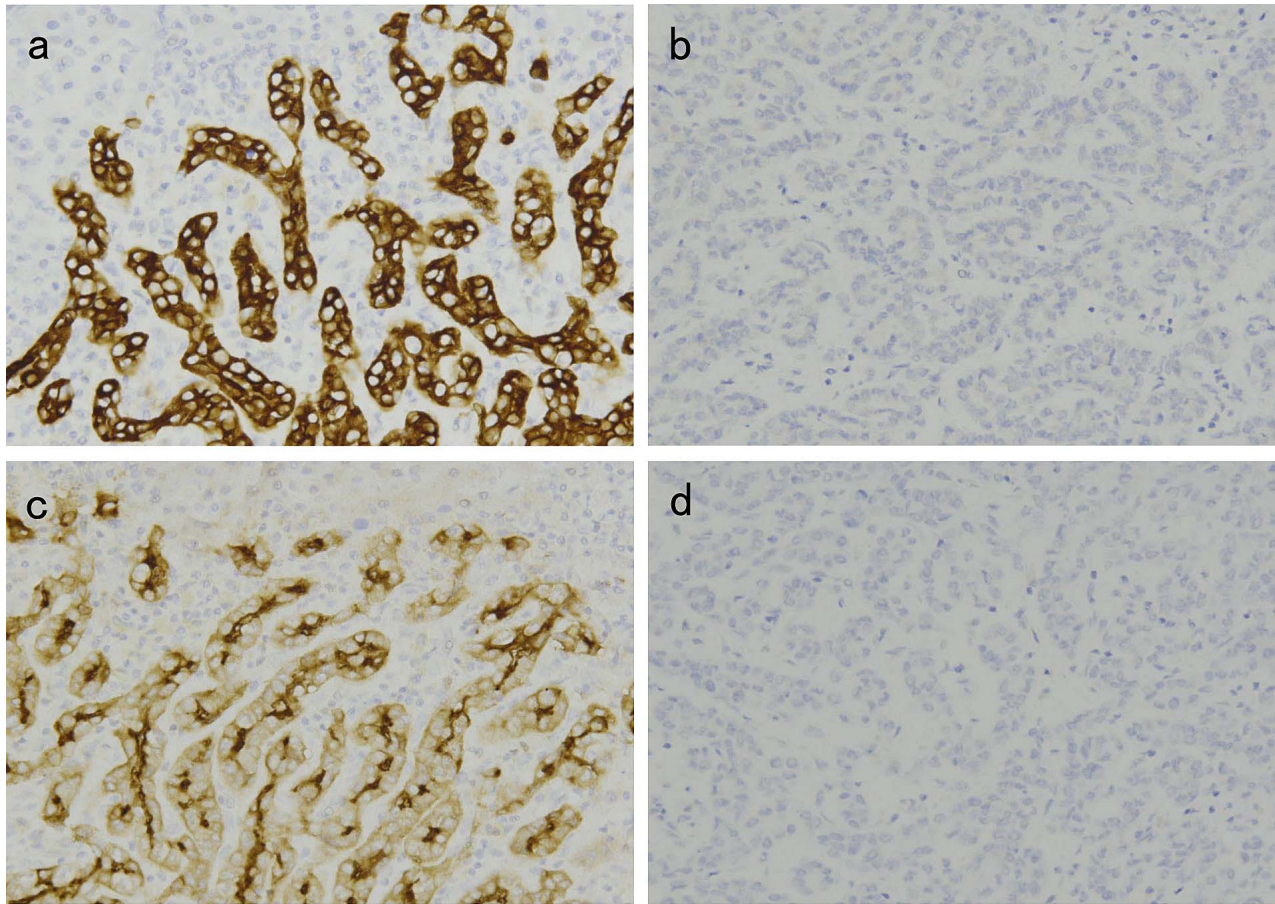


Fig. 6 Immunohistochemical staining of the tumor. The tumor cells were positive for cytokeratin (CK) 7 (a) and negative for CK 20 (b). Epithelial membrane antigen (EMA) was positive on the luminal surface of tubules of tumor cells (c). The tumor cells were negative for carcinoembryonic antigen (CEA) (d). Original magnification $\times 200$.

Conclusion

Preoperative diagnosis of CoCC was difficult because of its rarity, but recent data concerning imaging findings of CoCC have suggested its characteristic imaging features as mentioned already. Accordingly, we could strongly suspect a liver tumor preoperatively as CoCC, a rare liver tumor. In conclusion, cautious investigation of preoperative characteristic imaging findings possibly leads to accurate diagnosis of CoCC, despite its rarity.

Our article is a case report concerning one patient, and ethics approval was not required. Meanwhile, a written informed consent was obtained from the patient for publication of this case report and accompanying images.

References

1. Steiner PE, Higginson J. Cholangiolocellular carcinoma of the liver. *Cancer* 1959;**12**(4):753–759
2. Maeno S, Kondo F, Sano K, Takada T, Asano T. Morphometric and immunohistochemical study of cholangiolocellular carcinoma: comparison with non-neoplastic cholangiole, interlobular duct and septal duct. *J Hepatobiliary Pancreat Sci* 2012;**19**(3):289–296
3. Kondo F, Fukusato T. Pathogenesis of cholangiolocellular carcinoma: possibility of an interlobular duct origin. *Intern Med* 2015;**54**(14):1685–1694
4. Moeni A, Sia D, Zhang Z, Camprecios G, Stueck A, Dong H *et al*. Mixed hepatocellular cholangiocarcinoma tumors: cholangiolocellular carcinoma is a distinct molecular entity. *J Hepatol* 2017;**66**(5):952–961
5. Motosugi U, Ichikawa T, Nakajima H, Araki T, Matsuda M, Suzuki T *et al*. Cholangiolocellular carcinoma of the liver: imaging findings. *J Comput Assist Tomogr* 2009;**33**(5):682–688

6. Asayama Y, Tajima T, Okamoto D, Nishie A, Ishigami K, Ushijima Y *et al.* Imaging of cholangiolocellular carcinoma of the liver. *Eur J Radiol* 2010;**75**(1):e120–125
7. Kozaka K, Matsui O, Kobayashi S, Koda W, Minami T, Kitao A *et al.* Dynamic CT findings of cholangiolocellular carcinoma: correlation with angiography-assisted CT and histopathology. *Abdom Radiol (NY)* 2017;**42**(3):861–869
8. Haradome H, Unno T, Morisaka H, Toda Y, Kwee TC, Kondo H *et al.* Gadoteric acid disodium-enhanced MR imaging of cholangiolocellular carcinoma of the liver: imaging characteristics and histopathological correlations. *Eur Radiol* 2017;**27**(11):4461–4471
9. Theise ND, Nakashima O, Park YN, Nakanuma Y. Combined hepatocellular-cholangiocarcinoma. In: Bosman FT, Carneiro F, Hruban RH, Theise ND, eds. *WHO Classification of Tumors of the Digestive System*. Lyon, France: IARC Press, 2010:225–227
10. Kanamoto M, Yoshizumi T, Ikegami T, Imura S, Morine Y, Ikemoto T *et al.* Cholangiolocellular carcinoma containing hepatocellular carcinoma and cholangiocellular carcinoma, extremely rare tumor of the liver: a case report. *J Med Invest* 2008;**55**(1-2):161–165
11. Ishii N, Suzuki H, Tsukagoshi M, Watanabe A, Kubo N, Araki K *et al.* Giant cholangiolocellular carcinoma with early recurrence that was difficult to distinguish from cholangiocellular carcinoma: report of a case. *Int Surg* 2015;**100**(6):1111–1116
12. Suzumura K, Asano Y, Hirano T, Okada T, Uyama N, Aizawa N *et al.* Synchronous double cancers of primary hepatocellular carcinoma and cholangiolocellular carcinoma: a case report. *Surg Case Rep* 2016;**2**(1):139
13. Osawa M, Saitoh S, Fujiyama S, Kawamura Y, Sezaki H, Hosaka T *et al.* Cholangiolocellular carcinoma in a young patient who showed sustained virological response after treatment for hepatitis C virus infection. *Intern Med* 2017;**56**(22):3033–3040
14. Kadono M, Kimura K, Imamura J, Saeki S, Kurata M, Honda G *et al.* A case of a large cholangiolocellular carcinoma. *Clin J Gastroenterol* 2011;**4**(5):340–346
15. Takahashi Y, Sato S, Ishitobi H, Nagaoka M, Kobayashi Y, Fukuhara H *et al.* Intrahepatic cholangiolocellular and cholangiocellular carcinoma - differences in the 18F-FDG PET/CT findings. *Intern Med* 2017;**56**(22):3027–3031
16. Ishii N, Araki K, Yamanaka T, Handa T, Tsukagoshi M, Igarashi T, *et al.* Small cholangiolocellular carcinoma that was difficult to distinguish from cholangiocellular carcinoma: a case report. *Surg Case Rep* 2017;**3**(1):103
17. Mori N, Ichikawa T, Hashimoto J, Yamashita T, Yamada M, Hirabayashi K *et al.* Cholangiolocellular carcinoma of the liver exhibiting high F-18 FDG uptake. *Tokai J Exp Clin Med* 2016;**41**(2):60–64
18. Ariizumi S, Kotera Y, Katagiri S, Nakano M, Nakanuma Y, Saito A *et al.* Long-term survival of patients with cholangiolocellular carcinoma after curative hepatectomy. *Ann Surg Oncol* 2014;**21 Suppl 3**:S451–458
19. Chen J, He J, Deng M, Wu HY, Shi J, Mao L *et al.* Clinicopathological, radiologic, and molecular study of 23 combined hepatocellular-cholangiocarcinomas with stem cell features, cholangiolocellular type. *Hum Pathol* 2017;**64**:118–127
20. Yin X, Zhang BH, Qiu SJ, Ren ZG, Zhou J, Chen XH *et al.* Combined hepatocellular carcinoma and cholangiocarcinoma: clinical features, treatment modalities, and prognosis. *Ann Surg Oncol* 2012;**19**(9):2869–2876
21. Lee JH, Chung GE, Yu SJ, Hwang SY, Kim JS, Kim HY *et al.* Long-term prognosis of combined hepatocellular and cholangiocarcinoma after curative resection comparison with hepatocellular carcinoma and cholangiocarcinoma. *J Clin Gastroenterol* 2011;**45**(1):69–75
22. Jung DH, Hwang S, Hong SM, Chung YK, Song GW, Lee YJ *et al.* Post-resection prognosis of combined hepatocellular carcinoma-cholangiocarcinoma according to the 2010 WHO Classification. *World J Surg* 2017;**41**(5):1347–1357